Human primosome requires replication protein A when copying DNA with inverted repeats

Andrey G. Baranovskiy[1†], Lucia M. Morstadt[1†], Nigar D. Babayeva[1], Tahir H. Tahirov[1*]

[1]Eppley Institute for Research in Cancer and Allied Diseases, Fred & Pamela Buffett Cancer Center. University of Nebraska Medical Center, Omaha, NE, USA.

[†]These authors contributed equally to this work.

*To whom correspondence should be addressed. Email: ttahirov@unmc.edu

ABSTRACT

The human primosome, a four-subunit complex of primase and DNA polymerase alpha (Polα), initiates DNA synthesis on both chromosome strands by generating chimeric RNA-DNA primers for loading DNA polymerases delta and epsilon (Polε). Replication protein A (RPA) tightly binds to single-stranded DNA strands, protecting them from nucleolytic digestion and unauthorized transactions. We report here that RPA plays a critical role for the human primosome during DNA synthesis across inverted repeats prone to hairpin formation. On other alternatively structured DNA forming a G-quadruplex, RPA provides no assistance for primosome. A stimulatory effect of RPA on DNA synthesis across hairpins was also observed for the catalytic domain of Polα but not of Polε. The important factors for an efficient hairpin bypass by primosome are the high affinity of RPA to DNA based on four DNA-binding domains and the interaction of the winged-helix-turn-helix domain of RPA with Polα. Binding studies indicate that this interaction stabilizes the RPA/Polα complex on the primed template. This work provides insight into a cooperative action of RPA and primosome on DNA, which is critical for DNA synthesis across inverted repeats.

Keywords:

Primosome; DNA polymerase α; RPA; winged helix-turn-helix; hairpin; inverted repeats; G-quadruplex; DNA polymerase ε; protein-DNA interaction; protein-protein interaction; binding studies.

Abbreviations:

Polα – DNA polymerase α; Polα$_{CD}$ – catalytic domain of Polα; RPA – replication protein A; HP – hairpin; G4 – G-quadruplex; T:P - template:primer; aa – amino acid(s); ssDNA – single-stranded DNA; OB – oligonucleotide-binding; human CST – CTC1-STN1-TEN1; Polε – DNA polymerase ε.

INTRODUCTION

Human primosome is a multifunctional complex that plays a key role in genome replication (1,2). It initiates DNA synthesis at every origin of replication by generating chimeric RNA-DNA primers essential for recruiting two main replicases: DNA polymerase epsilon (Polε) and delta (Polδ) (3,4). Primosome is involved in a variety of other cellular processes, including telomere maintenance (5-7), genome stability (8-10), and innate immunity (11). It is an emerging candidate for antitumor therapy (12-14).

The human primosome is a complex of two enzymes: the two-subunit primase, with catalytic (p49) and regulatory (p58) subunits, and the two-subunit DNA polymerase α (Polα), with catalytic (p180) and accessory (p70) subunits (1,2). p180 contains a catalytic domain ($Pol\alpha_{CD}$) and a C-terminal domain ($p180_C$); p58 has N-terminal ($p58_N$) and C-terminal ($p58_C$) domains. Primosome forms an elongated platform p49-$p58_N$-$p180_C$-p70, which has some level of flexibility and holds $p58_C$ and $Pol\alpha_{CD}$ by linkers with a length of ~20 amino acid (aa) each (15-19). $Pol\alpha_{CD}$ adopts the universal "right-hand" DNA polymerase fold with an active site formed by a "palm" holding the catalytic aspartates, a "thumb" that binds the template:primer (T:P) duplex, and "fingers" interacting with an incoming nucleotide.

The primase is responsible for the initiation, elongation, and termination of RNA synthesis (1,20-22). We have shown that human primosome is structurally predetermined to synthesize the RNA primer with a length of nine nucleotides (16). Further primer extension by primase is inefficient due to a clash between $p58_C$ and $p58_N$. Owing to very low affinity of p49 to the primer 3'-end (23,24), Polα takes over the 9-mer RNA primer and extends it by ~25 deoxyribonucleotides (25,26). Structural modeling indicates that Polα cannot extend RNA primers shorter than 9-mer due to a clash between $p58_C$ and $Pol\alpha_{CD}$ (1). Importantly, $p58_C$ tightly binds to the primer 5'-end (24,26) and is a major regulator of all primosome transactions, also serving as a processivity factor for primase and Polα (16,19,27).

Replication protein A (RPA) is a hetero-trimeric protein with a conserved domain organization. RPA is a major single-stranded DNA (ssDNA)-binding protein in eukaryotes, which protects unwound DNA strands from nucleolytic damage and prevents reannealing and formation of alternate structures (28,29). RPA participates in a variety of DNA metabolic processes where ssDNA is involved, including DNA replication, DNA recombination, DNA repair, telomere maintenance and the DNA damage response, and checkpoint activation (30). The recent study utilizing reconstituted reactions with yeast proteins have shown that RPA is critical for origin unwinding and DNA replication (31).

Human RPA is composed of three subunits: RPA70, RPA32, and RPA14 (Fig. 1), and contains six oligonucleotide-binding (OB)-domains (F, A, B, C, D, and E), with four of them (A-D) being involved in ssDNA-binding (29). RPA is composed of two main modules flexibly connected: N-terminal (domains F, A, and B) and C-terminal (RPAcore; contains both small subunits and the C domain of RPA70). A zinc-binding motif is a part of C-domain and is important for structural stability and DNA binding (32,33). Besides DNA binding, C and D also participate in intersubunit interactions, together with RPA14 (OB-fold E) forming a minimal trimerization core ($RPAcore^{\Delta P,W}$) (34). The N-terminus of RPA32 (P-motif; residues 1-33) undergoes phosphorylation in response to cell cycle progression and DNA damaging agents, however the structural and functional impact of this modification is not well understood (35). The C-terminus of RPA32 contains a flexibly tethered winged helix-turn-helix domain (wHTH, shortly W; residues 203-270), which interacts with different DNA processing proteins with relatively low affinity (K_D in the range of 5-10 μM) (36,37). The N-terminal part of RPA70 also mediates RPA interaction with several binding partners, including viral proteins (29).

RPA binds ssDNA with high affinity, with K_D values in sub-nanomolar range (38). In the compact DNA-binding mode, RPA bends ssDNA in a horseshoe-like configuration (Fig. 1) (39). According to that structure, the AB-domains and RPAcore interact with 8 and 17 nucleotides, respectively, which is consistent with structural information for the A/B domains in complex with an 8-mer ssDNA (40). RPA binds ssDNA with a defined 5'→3' polarity, with small subunits facing the T:P junction (41). Of note, RPAcore retains the ability to recognize DNA polarity (42). An interaction between RPA and primosome was detected more than thirty years ago using enzyme-linked immunoassay (43). Later, a more elaborated study have shown that the W-domain plays an important role in RPA-Polα interaction (44). Currently, no structural information is available for the entire RPA-primosome complex as well as for its separate parts.

In this work, we have shown that RPA has a strong stimulatory effect on primosome and $Pol\alpha_{CD}$ upon DNA synthesis across inverted repeats. We conducted a series of biochemical experiments along with analysis of current structural information to gain insight into the mechanism of Polα activity modulation by RPA. Several RPA mutants were generated to study the role of RPA domains on activity of Polα alone and in the complex with primase, depending on DNA template structure. Binding studies were conducted to explore the role of the W-domain in stabilization of the RPA/Polα/DNA complex. Altogether, our studies revealed the importance of cooperation between RPA and Polα during DNA synthesis across inverted repeats.

RESULTS

RPA facilitates DNA synthesis termination by primosome

To analyze the effect of RPA and DNA secondary structures on primosome activity we used a recently published assay, utilizing a natural primer (26). In this assay, Polα extends the primer 3'-end while the primase accessory subunit holds the primer 5'-end. Primosome and RPA were pre-incubated with a 98-mer DNA template annealed to a 12-mer chimeric RNA-DNA primer (5'-ppp*GGCGGCACG*ACC, RNA region is in italics, Supplementary Table 1), and DNA synthesis was initiated by addition of 10 μM dNTPs. The length of the 5'-tail is 81 nucleotides, allowing at least two RPA molecules to bind it.

In primosome, the tight complex between the primase and the primer 5'-end allows Polα to perform processive DNA synthesis on the unstructured template (Fig. 2, lanes 1 and 2). On the other hand, simultaneous primer binding at the 5'-end by primase and at the 3'-end by Polα sets a limit for the length of a chimeric RNA-DNA primer, which is defined by two primosome linkers. Recently, we have shown that at single-turnover conditions, the primosome mainly generates 32-35-mer primers (19,26). In the absence of RFC and DNA polymerases δ and ε, which compete with Polα for the primer 3'-end *in vivo*, Polα is able to add several extra nucleotides due to further stretching of the linkers.

On the unstructured (normal) template, RPA exhibits an inhibitory effect on DNA synthesis (Fig. 2, lanes 1-4). Seemingly, RPA tightly bound to DNA should be an obstacle for any of the DNA polymerases, which utilize the energy of phosphodiester bond hydrolysis to displace RPA from a template. Interestingly, RPA reduces the level of products with a length exceeding 32 nucleotides (Fig. 2, lanes 1-4). This observation indicates that RPA prevents Polα from resuming DNA synthesis and is an additional factor in the composite mechanism of DNA synthesis termination by primosome (19,26), which limits the amount of mutagenic DNA generated by Polα (8,45). As we shown in previous studies, a tension in primosome linkers makes more difficult for Polα to rebind the mature 35-mer primer and continue DNA synthesis (19,26). It seems obvious that Polα dissociation from DNA will result in disruption of a dynamic complex RPA-Polα, allowing RPA to move closer to the primer 3'-end, which will further complicate Polα rebinding.

RPA helps primosome in bypassing a hairpin but not a G-quadruplex

Next, we analyzed how RPA modulates primosome activity on alternatively structured DNA, which usually presents a challenge for DNA-processing proteins (46-48). In the template, structured

DNA elements were placed nine nucleotides apart from the primer 3'-end, to clearly observe primosome stalling at the obstacle before DNA synthesis termination at the 32-mer product. A stable hairpin (HP) with a 9-bp stem completely stalls the primosome (Fig. 2, lanes 5 and 6). Strikingly, RPA greatly stimulates HP bypass by the primosome (Fig. 2, lanes 7 and 8).

The other known replication block tested in this work was the G-quadruplex (G4) motif, which folds into a four-stranded structure composed of stacked guanine tetrads (49). G4 motifs are positioned non-randomly in the genome and usually locate at telomeres, origins of replication, sites of recombination, and in gene promoter regions, including promoters of many oncogenes. The G4-forming motif stalls primosome (Fig. 2, lanes 9 and 10) but to a smaller extent than HP. Surprisingly, RPA does not help primosome to bypass a G4 structure (lanes 11 and 12).

It is known that RPA can passively unfold hairpins and G4 structures by stabilizing the unfolded state (50-53). The failure of RPA to help Polα in DNA synthesis across a G4 motif can be attributed to the high stability of the G-quadruplex, resulting in a slow unfolding rate (54,55). In addition, partial RPA displacement by Polα during G4 bypass should reduce RPA affinity to DNA and its ability to stabilize an unfolded G4 motif. It is possible that additional factors are required for primosome to perform efficient DNA synthesis across a G4 motif. It is known that another ssDNA-binding protein CTC1-STN1-TEN1 (CST) helps primosome to copy the G-strand of telomeric DNA, which contains G4 motifs (56-58).

The W-domain is required for the hairpin bypass by primosome

Using an enzyme-linked immunosorbent assay, it was shown that the W-domain deletion disrupts the RPA-Polα interaction (44). The deleted region (residues 223-270) is a part of the W-domain (Fig. 1), which is flexibly connected to the rest of RPA and does not participate in the interaction with DNA. This domain mediates RPA interaction with different proteins, including the DNA recombination protein Rad52, the DNA repair proteins XPA and uracil DNA glycosylase 2, and the T-antigen of polyomavirus SV40 (29).

We generated an RPA variant named $RPA^{\Delta W}$ (Fig. 1 and Supplementary Fig. 1) by deleting the region 175-270, which contains the W-domain and the linker connecting it to the rest of RPA32. This deletion almost completely abrogated the stimulatory effect of RPA on HP bypass by primosome (Fig. 3A, lanes 3 and 4). These data show the critical role of the W-domain in DNA synthesis across HP by primosome. Of note, a W-domain deletion slightly increased the inhibitory effect of RPA on

unstructured DNA (Fig. 3A, lanes 1 and 2, in comparison to Fig. 2, lanes 3 and 4), indicating that the W-Polα interaction helps Polα to displace RPA from a template as DNA synthesis proceeds. Consistently, the recent study utilizing *in vitro* reconstituted DNA replication reactions with yeast proteins, showed a stimulatory role of the W-domain on the leading and lagging strands synthesis (31).

RPAcore stimulates DNA synthesis but not a hairpin bypass

It should be expected that the tight RPA-DNA interaction, which requires all four DNA-binding domains, is important for stabilizing unfolded hairpins and, therefore, for efficient HP bypass by the primosome/RPA complex. To test this idea, we generated the RPA variant RPAcore$^{\Delta P}$ by deleting the N-terminal part of RPA70 (residues 1-437), as well as the disordered N-terminus of RPA32 (P-motif; residues 1-34), whose function is not well characterized except that it becomes phosphorylated after DNA damage (35). The P-motif deletion allowed to significantly increase the protein yield after purification.

RPAcore$^{\Delta P}$ almost completely lost the ability to stimulate the HP bypass (Fig. 3A, lanes 5 and 6). Interestingly, on unstructured DNA, it shows the opposite effect versus the wild-type RPA (Fig. 3A, lanes 7 and 8, in comparison to Fig. 2, lanes 3 and 4), stimulating the DNA-polymerase activity. This fact supports the idea that high RPA affinity to DNA complicates its displacement by DNA polymerase.

We created two derivatives of RPAcore$^{\Delta P}$, one with intact RPA32 (named RPAcore) and the other with an additionally deleted W-domain (named RPAcore$^{\Delta P,W}$), which represents a minimal trimerization core composed of domains C, D, and E (34). In comparison to RPAcore$^{\Delta P}$, RPAcore shows similar effect on primosome on both DNA templates (Fig. 3B, lanes 2-5), with a somewhat reduced stimulatory effect on the unstructured template. RPAcore$^{\Delta P,W}$, missing the W-domain, shows a complete loss of ability to stimulate primosome activity on HP and a normal template (Fig. 3B, lanes 6-9). Thus, the stimulatory effect of RPA on HP bypass by primosome is based on high affinity of RPA to DNA and the W-domain.

The catalytic domain of Polα depends on the W-domain of RPA upon DNA synthesis across a hairpin

Next, we decided to check whether Polα$_{CD}$ exhibits a similar dependence on RPA upon DNA synthesis across HP, as was observed for primosome. A previously published assay was employed where Polα$_{CD}$ extends a 16-mer DNA primer annealed to a 73-mer template (59). On a normal template,

Polα_{CD} generates a significant amount of a 70-mer primer in 1 min (Fig. 4A, lane 2). In contrast to the primosome assay, DNA synthesis termination at the primer length of ~35nt is not observed, due to the absence of the primase accessory subunit and the triphosphate group on the primer (26). Polα_{CD} displays the same behavior on HP and G4 templates as primosome, making a pronounced pause at these structures (Fig. 4A, lanes 6, 7, 10, and 11). RPA does not stimulate Polα_{CD} on the normal template (Fig. 4A, lanes 2-5), but it provides a remarkable assistance upon DNA synthesis across HP (lanes 6-9). As with primosome, RPA does not help Polα_{CD} on the G4 template (Fig. 4A, lanes 10-13).

In addition, we analyzed the effect of two RPA derivatives, RPAcore and RPA$^{\Delta W}$, on the Polα_{CD} activity on the normal and HP templates. Both truncations severely affected the ability of RPA to stimulate Polα_{CD} during HP bypass (Fig. 4B, lanes 3, 4, 7, and 8, in comparison to Fig. 4A, lanes 8 and 9). These results indicate that in primosome, Polα makes the most important contacts with RPA.

The W-domain stabilizes the RPAcore/DNA/Polα complex

We employed Bio-Layer Interferometry to determine the role of the W-domain in the interaction of RPA with DNA and Polα. This approach allows for obtaining the rate constants of complex formation (k_{on}), dissociation (k_{off}), and the dissociation constant (K_D) can be obtained. The intact RPA with all four DNA-binding domains is not suitable for this assay due to very tight DNA binding, which results in hours-long dissociation and notable ageing of solutions. In this regard, we used RPA variants with the deleted N-terminal part of RPA70 containing DNA-binding domains A and B. These domains are more dynamic on ssDNA with faster on-off kinetics in comparison to RPAcore (60). A pre-annealed T:P with a biotin at the 5′-tail of a template (Supplementary Table 1) was loaded on a streptavidin biosensor and dipped into solutions containing RPA variants at different concentrations. The binding studies were conducted at near-physiological salt composition (61).

First, we determined an affinity of RPAcore$^{\Delta P,W}$ to a 35-mer template duplexed with an 11-mer primer (template makes a 24-mer 5'-tail) and obtained a K_D value of 90 nM (Table 1). Next, we analyzed the effect of Polα on the RPAcore$^{\Delta P,W}$/DNA interaction. The DNA sensor was preloaded with Polα_{CD} in one well and then moved to the well containing RPAcore$^{\Delta P,W}$ in addition to the same concentration of Polα_{CD}, so that the interaction of the RPAcore variant with DNA/Polα could be analyzed (Fig. 5A). Strikingly, the K_D value increased by almost 30-fold (up to 2.5 μM), which was mainly due to the more than 10-fold increase of a k_{off} value (Table 1). This result points to a competition between Polα_{CD} and RPAcore$^{\Delta P,W}$ upon T:P binding.

In comparison to RPAcore$^{\Delta P,W}$, the variant with an intact W-domain (RPAcore$^{\Delta P}$) showed slightly lower affinity to T:P (K_D = 124 nM, Table 1). This result indicates that the W-domain does not participate in the interaction with DNA. Remarkably, in the presence of Polα$_{CD}$, affinity of this RPA variant to DNA increased 2.5-fold (K_D = 50 nM), with a 5-fold reduction of the k_{off} value, which is inversely proportional to the complex stability (Table 1, binding kinetics are shown on Fig. 5B). Thus, the W-domain causes a switch in the cooperativity between RPAcore and Polα, turning it from negative to positive, and providing a ~50-fold gain in stability of the RPAcore/Polα/DNA complex. Probably, this complex exists *in vivo* when A/B-domains are displaced from DNA by moving primosome (see Discussion).

A stimulatory effect of human Polα on the RPAcore-DNA interaction is in agreement with studies conducted with yeast proteins showing that RPA stabilizes the Polα/DNA complex (62). Indeed, in the ternary complex RPA/Polα/DNA, each component should be critical for its stability. Of note, the CST/Polα complex is not stable without DNA, which acts as a "glue" for the complex (56,63).

RPA does not assist human Polε$_{CD}$ during DNA synthesis across a hairpin

For comparison, we analyzed the effect of RPA on activity of the catalytic domain of human DNA polymerase ε (Polε$_{CD}$) under the same conditions as for Polα$_{CD}$. Polε is specialized in the synthesis of the leading strand, has a potent 3'→5' exonuclease activity, and works in the complex with a CMG helicase (64-66). As for Polα and the primosome, HP and G4 structures present a strong obstacle for Polε$_{CD}$ (Fig. 6). The pausing of DNA synthesis on HP and G4 templates was previously reported for yeast Polε (67) and human Polε$_{CD}$ (68), respectively.

Strikingly, RPA does not help Polε$_{CD}$ in bypassing HP and shows an inhibitory effect on both normal and structured templates. It is clear that RPA is able to unfold HP ahead of Polε, as was observed in reactions with Polα, and that Polε$_{CD}$ is able to displace RPA (Fig. 6, lanes 1-4), but somehow RPA does not help Polε to bypass the HP motif. This fact points to the importance of cooperation between a DNA polymerase and RPA upon template handover between them.

Of note, HP and especially G4 increase the level of products with a length below 16 nucleotides (Fig. 6, lanes 5, 6, 9, and 10, in comparison to lanes 1 and 2), which indicates the shift in the balance of polymerase/exonuclease activities toward the latter. Interestingly, RPA stimulates the exonuclease activity of Polε$_{CD}$ on the HP template but inhibits on the G4 template (Fig. 6, lanes 5-12). A possible explanation is that RPA unfolds G4 less efficiently and cannot bind tightly to the short stretch of a

template between G4 and the primer, which reduces an inhibitory effect of RPA on DNA polymerizing activity.

DISCUSSION

Our studies uncovered a critical role of RPA in DNA synthesis across hairpins by primosome. In contrast to CST, RPA does not help primosome at the other alternatively structured DNA, a G-quadruplex. This fact may indicate that, besides RPA, additional factors are required for primosome to bypass this obstacle, or that mainly CST assists primosome at G4 motifs, especially during a C-strand extension at telomeres. RPA does not stimulate a DNA-polymerase activity of primosome on the unstructured template when using a native-like RNA-DNA primer with a 5'-triphosphate. The important factors required for RPA-assisted hairpin bypass by Polα are high affinity of RPA to DNA and an interaction of the W-domain with the catalytic domain of Polα.

Cooperation between RPA and primosome during DNA synthesis across HP indicates that RPA can deliver unfolded DNA directly to the Polα active site. The recently reported structure of human CST in complex with primosome and ssDNA revealed the shared DNA binding by Polα and CST, which together completely encircle the DNA strand (56,57). Similar structural organization of ssDNA-binding proteins CST and RPA, which are hetero-trimers with four DNA-binding domains, suggests a common mode of DNA binding by CST/Polα and RPA/Polα (56,69). To check this hypothesis, we performed the structural alignment, which shows a good fit between RPAcore and the corresponding OB domains of CST (Fig. 7A). Moreover, high similarity in organization of DNA-binding clefts, facing Polα, was unveiled (Fig. 7B). This analysis support the idea that RPA (in particular, the C-domain), engages with Polα/DNA in a similar way as was observed for CST (56,57), which might be an additional factor contributing to efficient hairpin bypass.

This study have shown that the interaction between Polα and the W-domain of RPA dramatically increases cooperativity between RPAcore and Polα upon T:P binding and promotes hairpin bypass by the RPA/primosome and RPA/Polα complexes. Strikingly, the structure of the CST/Polα/DNA complex allowed us to predict the interaction site for the W-domain on $Pol\alpha_{CD}$. According to that structure, the second wHTH domain of STN1 establishes a small interaction interface with an α-helix of $Pol\alpha_{CD}$ (residues 615-629) (56). The W-domain of RPA aligns very well with the second wHTH of STN1, especially near the Polα interaction site (Supplementary Fig. 2). Moreover, the same RPA32-binding site composed of an α-helix was reported for DNA repair proteins uracil-DNA glycosylase UNG2 and a

helicase SMARCAL1 (36,70). Of note, the linker connecting the N- and C-terminal parts of STN1 is distant from DNA and Polα (56).

This work provides a clue to which order RPA domains are displaced from a template as DNA synthesis progresses. RPAcore binds to Polα/DNA with higher affinity than the A/B-domains bind to DNA (K_D values are 50 nM (Table 1) and 114 nM (71), respectively). Interestingly, in the cryoEM structure of yeast RPA complexed with 100-mer ssDNA, only RPAcore is visible in complex with DNA (72), which points to a more stable DNA-binding, even without Polα. Decreased stability of the A/B/DNA complex is probably due to the flexible connection of DNA-binding domains A and B, each having a one to two orders of magnitude lower affinity to DNA in comparison to their tandem (71). According to these data, we suggest that the N-terminal part of RPA70 is displaced from ssDNA first, probably, as a result of sequential displacement of A- and B-domains.

To approximate the trajectory of DNA between RPA and Polα, $Pol\alpha_{CD}$ in complex with T:P as well as RPA/ssDNA were aligned to CST/Primosome/ssDNA where Polα is in apo-form (Supplementary Fig. 3A). This alignment revealed the position of a thumb domain, which became stabilized upon T:P binding and could make additional contacts with CST or RPA. The distance between the 3'-end of DNA in complex with RPA and the 5'-end of a DNA template in complex with $Pol\alpha_{CD}$ is 35 Å (Supplementary Fig. 3B). This means that more than six nucleotides are required for the DNA linker between RPA and Polα, with a sharp turn at RPA. Polα pulls a DNA template upon synthesis. It is possible that the four nucleotides of ssDNA that do not interact with Polα, according to the structure of the complex CST/Primosome/DNA (56), are detached from RPA, resulting in a shorter DNA path between Polα and RPA and to a smoother DNA turn at RPA (Supplementary Fig. 3C).

Our data point to a different mode of RPA interaction with Polε versus Polα or to the absence of interaction. Structural analysis indicates that Polε cannot interact with RPA/DNA in the same way as Polα because of a clash between the processivity domain of Polε and the D-domain of RPA (Supplementary Fig. 4). RPA might be of little importance for Polε because it receives the parental DNA strand directly from CMG. There is also a possibility that RPA-Polε interaction is mediated by the other replication factors like PCNA (73).

MATERIALS AND METHODS

Oligonucleotides for functional studies

Sequences of all oligonucleotides are provided in Supplementary Table 1. Oligonucleotides were obtained from IDT Inc. A 12-mer chimeric RNA-DNA primer (P1) was obtained by ligation as described elsewhere (26).

Protein expression and purification

Purification of the human primosome and the Polα catalytic core have been described elsewhere (59). As previously reported, the N-terminus of p180 (residues 1-334) has been deleted because it is poorly folded and is not required for activity (19,56). Purification to homogeneity of the catalytic domain of human Polε (Polε_{CD}, residues 28-1194) was conducted according to (74).

Genes encoding three subunits of human RPA were cloned into pASHSUL-1 plasmid (75), resulting a poly-cistronic expression vector with the following order of subunits: RPA70, RPA32, and RPA14. A cleavable His-Sumo-tag was placed at the N-terminus of RPA70. RPA truncation variants were obtained according to (76). Human RPA and its variants were expressed in *Escherichia coli* strain BL21 (DE3) at 16 ºC for 15 hours following induction with 0.3 µg/ml anhydrotetracyclin. Afterward, cells were harvested by centrifugation at 4,000 g for 15 min, aliquoted, and kept at -80 ºC.

All RPA variants were purified according to the same protocol, including chromatography on a Ni-IDA column (Bio-Rad), His-Sumo tag digestion during overnight incubation on ice, and two additional chromatographic steps using Heparin HP HiTrap and monoQ 5/50 GL columns (Cytiva). Finally, samples were concentrated and flash-frozen in aliquots. The purity of samples was analyzed by SDS-PAGE (Supplementary Fig. 1). Protein concentrations were estimated by measuring the absorbance at 280 nm and using the extinction coefficients calculated with ProtParam (77).

Primosome activity assay

DNA-synthetic activity of primosome was tested in a 10 µl reaction containing 0.2 µM T:P, 0.2 µM enzyme, 1µM RPA or its variants, 10 µM dNTPs, 0.1 µM [α-^{32}P]-dCTP (3000 Ci/mmol; PerkinElmer, Inc.), and the buffer: 30 mM Tris-Hepes, pH 7.8, 120 mM KCl, 30 mM NaCl, 1% glycerol, 1.5 mM TCEP, 5 mM $MgCl_2$, and 0.2 mg/ml BSA. The proteins were pre-incubated with T:P for 1 min on ice and for 10 sec at 35 ºC, then reaction was initiated by addition of the equal volume of buffer solution containing dNTPs. Reactions were incubated in PCR tubes on a water bath for the indicated time points at 35 °C and stopped by mixing with equal volume of formamide loading buffer (90% v/v formamide, 50 mM EDTA, pH 8, 0.02% Bromophenol blue), heated at 95 °C for 1 min, and

resolved by 20% Urea-PAGE (UreaGel System (19:1 Acrylamide/Bisacrylamide), National Diagnostics) for 2.5 h at 3000 V. The reaction products were visualized by phosphorimaging (Typhoon FLA 9500, Cytiva). Experiments were repeated three times.

DNA polymerase activity assay

DNA-synthetic activity of Polα_{CD} and Polε_{CD} was tested in a 10 µl reaction containing 0.25 µM T:P, 20 nM enzyme, 1µM RPA or its variants, 50 µM dNTPs, and the buffer: 30 mM Tris-Hepes, pH 7.8, 120 mM KCl, 30 mM NaCl, 1% glycerol, 1.5 mM TCEP, 5 mM $MgCl_2$, and 0.2 mg/ml BSA. A 16-mer DNA primer contains a Cy5 fluorophore attached to the 5'-end. RPA was pre-incubated with T:P and dNTPs for 1 min on ice and for 10 sec at 35 ºC, then reaction was initiated by addition of the equal volume of buffer solution containing enzyme. Reactions were incubated in PCR tubes on a water bath for the indicated time points at 35 °C and stopped by mixing with equal volume of formamide loading buffer (90% v/v formamide, 50 mM EDTA, pH 8, 0.02% Bromophenol blue), heated at 95 °C for 1 min, and resolved by 20% Urea-PAGE (UreaGel System (19:1 Acrylamide/Bisacrylamide), National Diagnostics). The reaction products were visualized by imaging on Typhoon FLA 9500 (Cytiva). Experiments were repeated three times.

Binding studies

Analysis of binding kinetics was done at 23 ºC using Octet K2 (Sartorius AG), as previously described (61). This device uses Bio-Layer Interferometry technology to monitor molecular interactions in real time. The 35-mer template with a biotin-TEG at the 5'-overhang was annealed to an 11-mer primer (Supplementary Table 1) and immobilized on a streptavidin-coated biosensor (SAX, Sartorius AG). A chimeric RNA-DNA primer demonstrating the highest affinity to Polα (45) was utilized in order to saturate DNA sensors with Polα_{CD} at the minimal concentration. Dideoxy-cytidine was placed at the primer 3′-end to prevent DNA polymerase reaction. SAX sensors were loaded with oligonucleotide-biotin at 50 nM concentration for 7 min at 500 rpm, then sensors were blocked by incubating with 10 µg/ml biocytin for 2 min.

Binding studies were conducted in a 96-well microplate (Greiner Bio-One) in buffer containing 25 mM Tris-Hepes, pH 7.8, 120 mM KCl, 30mM NaCl, 2.5 mM $MgCl_2$, 50 µM dTTP, 2 mM TCEP, and 0.002% Tween-20. The first six wells in a row contained only the buffer, and the next six wells contained two-fold dilutions of RPA variant in the same buffer. Before and after incubation with RPA

(association step), the DNA-sensor was placed into the same RPA-free well (distinct for each RPA concentration), resulting in baseline and dissociation steps, respectively.

Upon binding studies in the presence of Polα_{CD}, the DNA sensor was moved first to the well containing 100 nM Polα_{CD}. The next well, where the association step was carried out, contained an RPA variant as well as 100 nM Polα_{CD} to maintain an equilibrium between sensor-bound and free Polα_{CD}. To observe dissociation of an RPA variant from the Polα/DNA complex, a sensor was moved to the same well where it was pre-loaded with Polα_{CD}. RPAcore and its variant containing a W-domain were used at concentrations of 3.6 μM and 200 nM, respectively, exceeding the corresponding K_D values. Data Analysis HT software (ver. 11.1, Sartorius AG) was used for calculation of binding constants (k_{on}, k_{off}, and K_D). The average value and standard deviation were calculated from three independent experiments.

Supplementary material description

Table 1. Oligonucleotides used in this study.

Figure 1. Analysis of purity of human RPA and its variants.

Figure 2. The alignment of a W-domain of RPA with a second wHTH domain of CST.

Figure 3. Approximation of a DNA path between Polα and RPA.

Figure 4. Polε cannot interact with RPA/DNA in the same way as Polα.

Acknowledgements

This work was supported by the National Institute of General Medical Sciences grant R35GM152032 to T.H.T. We thank K. Jordan for editing this manuscript.

Conflict of interest statement. None declared

REFERENCES

1. Baranovskiy, A.G. and Tahirov, T.H. (2017) Elaborated Action of the Human Primosome. *Genes (Basel)*, **8**.
2. Pellegrini, L. (2012) The Pol alpha-primase complex. *Subcell Biochem*, **62**, 157-169.
3. Burgers, P.M.J. and Kunkel, T.A. (2017) Eukaryotic DNA Replication Fork. *Annu Rev Biochem*, **86**, 417-438.
4. Pellegrini, L. and Costa, A. (2016) New Insights into the Mechanism of DNA Duplication by the Eukaryotic Replisome. *Trends Biochem Sci*, **41**, 859-871.
5. Casteel, D.E., Zhuang, S., Zeng, Y., Perrino, F.W., Boss, G.R., Goulian, M. and Pilz, R.B. (2009) A DNA polymerase-{alpha}{middle dot}primase cofactor with homology to replication protein A-32 regulates DNA replication in mammalian cells. *J Biol Chem*, **284**, 5807-5818.
6. Mizuno, T., Hirabayashi, K., Miyazawa, S., Kobayashi, Y., Shoji, K., Kobayashi, M., Hanaoka, F., Imamoto, N. and Torigoe, H. (2021) The intrinsically disordered N-terminal region of mouse DNA polymerase alpha mediates its interaction with POT1a/b at telomeres. *Genes Cells*, **26**, 360-380.
7. Zaug, A.J., Goodrich, K.J., Song, J.J., Sullivan, A.E. and Cech, T.R. (2022) Reconstitution of a telomeric replicon organized by CST. *Nature*, **608**, 819-825.
8. Reijns, M.A.M., Kemp, H., Ding, J., de Proce, S.M., Jackson, A.P. and Taylor, M.S. (2015) Lagging-strand replication shapes the mutational landscape of the genome. *Nature*, **518**, 502-506.
9. Schimmel, J., Munoz-Subirana, N., Kool, H., van Schendel, R. and Tijsterman, M. (2021) Small tandem DNA duplications result from CST-guided Pol alpha-primase action at DNA break termini. *Nat Commun*, **12**, 4843.
10. Mirman, Z., Lottersberger, F., Takai, H., Kibe, T., Gong, Y., Takai, K., Bianchi, A., Zimmermann, M., Durocher, D. and de Lange, T. (2018) 53BP1-RIF1-shieldin counteracts DSB resection through CST- and Polalpha-dependent fill-in. *Nature*, **560**, 112-116.
11. Starokadomskyy, P., Gemelli, T., Rios, J.J., Xing, C., Wang, R.C., Li, H., Pokatayev, V., Dozmorov, I., Khan, S., Miyata, N. *et al.* (2016) DNA polymerase-alpha regulates the activation of type I interferons through cytosolic RNA:DNA synthesis. *Nat Immunol*, **17**, 495-504.
12. Han, T., Goralski, M., Capota, E., Padrick, S.B., Kim, J., Xie, Y. and Nijhawan, D. (2016) The antitumor toxin CD437 is a direct inhibitor of DNA polymerase alpha. *Nat Chem Biol*, **12**, 511-515.
13. Dallavalle, S., Musso, L., Cincinelli, R., Darwiche, N., Gervasoni, S., Vistoli, G., Guglielmi, M.B., La Porta, I., Pizzulo, M., Modica, E. *et al.* (2022) Antitumor activity of novel POLA1-HDAC11 dual inhibitors. *Eur J Med Chem*, **228**, 113971.
14. Abdel-Samad, R., Aouad, P., Gali-Muhtasib, H., Sweidan, Z., Hmadi, R., Kadara, H., D'Andrea, E.L., Fucci, A., Pisano, C. and Darwiche, N. (2018) Mechanism of action of the atypical retinoid ST1926 in colorectal cancer: DNA damage and DNA polymerase alpha. *Am J Cancer Res*, **8**, 39-55.
15. Baranovskiy, A.G., Zhang, Y., Suwa, Y., Babayeva, N.D., Gu, J., Pavlov, Y.I. and Tahirov, T.H. (2015) Crystal structure of the human primase. *J Biol Chem*, **290**, 5635-5646.
16. Baranovskiy, A.G., Babayeva, N.D., Zhang, Y., Gu, J., Suwa, Y., Pavlov, Y.I. and Tahirov, T.H. (2016) Mechanism of Concerted RNA-DNA Primer Synthesis by the Human Primosome. *J Biol Chem*, **291**, 10006-10020.
17. Kilkenny, M.L., Veale, C.E., Guppy, A., Hardwick, S.W., Chirgadze, D.Y., Rzechorzek, N.J.,

Maman, J.D. and Pellegrini, L. (2022) Structural basis for the interaction of SARS-CoV-2 virulence factor nsp1 with DNA polymerase alpha-primase. *Protein Sci*, **31**, 333-344.

18. Nunez-Ramirez, R., Klinge, S., Sauguet, L., Melero, R., Recuero-Checa, M.A., Kilkenny, M., Perera, R.L., Garcia-Alvarez, B., Hall, R.J., Nogales, E. *et al.* (2011) Flexible tethering of primase and DNA Pol alpha in the eukaryotic primosome. *Nucleic Acids Res*, **39**, 8187-8199.
19. He, Q., Baranovskiy, A.G., Morstadt, L.M., Lisova, A.E., Babayeva, N.D., Lusk, B.L., Lim, C.J. and Tahirov, T.H. (2023) Structures of human primosome elongation complexes. *Nat Struct Mol Biol*, **30**, 579-583.
20. Sheaff, R.J. and Kuchta, R.D. (1993) Mechanism of calf thymus DNA primase: slow initiation, rapid polymerization, and intelligent termination. *Biochemistry*, **32**, 3027-3037.
21. Copeland, W.C. and Wang, T.S. (1993) Enzymatic characterization of the individual mammalian primase subunits reveals a biphasic mechanism for initiation of DNA replication. *J Biol Chem*, **268**, 26179-26189.
22. Kuchta, R.D., Reid, B. and Chang, L.M. (1990) DNA primase. Processivity and the primase to polymerase alpha activity switch. *J Biol Chem*, **265**, 16158-16165.
23. Cordoba, J.J., Mullins, E.A., Salay, L.E., Eichman, B.F. and Chazin, W.J. (2023) Flexibility and Distributive Synthesis Regulate RNA Priming and Handoff in Human DNA Polymerase alpha-Primase. *J Mol Biol*, **435**, 168330.
24. Baranovskiy, A.G., Zhang, Y., Suwa, Y., Gu, J., Babayeva, N.D., Pavlov, Y.I. and Tahirov, T.H. (2016) Insight into the Human DNA Primase Interaction with Template-Primer. *J Biol Chem*, **291**, 4793-4802.
25. Murakami, Y., Eki, T. and Hurwitz, J. (1992) Studies on the initiation of simian virus 40 replication in vitro: RNA primer synthesis and its elongation. *Proc Natl Acad Sci U S A*, **89**, 952-956.
26. Baranovskiy, A.G., Lisova, A.E., Morstadt, L.M., Babayeva, N.D. and Tahirov, T.H. (2022) Insight into RNA-DNA primer length counting by human primosome. *Nucleic Acids Res*, **50**, 6264-6270.
27. Zerbe, L.K. and Kuchta, R.D. (2002) The p58 subunit of human DNA primase is important for primer initiation, elongation, and counting. *Biochemistry*, **41**, 4891-4900.
28. Chen, R. and Wold, M.S. (2014) Replication protein A: single-stranded DNA's first responder: dynamic DNA-interactions allow replication protein A to direct single-strand DNA intermediates into different pathways for synthesis or repair. *Bioessays*, **36**, 1156-1161.
29. Fanning, E., Klimovich, V. and Nager, A.R. (2006) A dynamic model for replication protein A (RPA) function in DNA processing pathways. *Nucleic Acids Res*, **34**, 4126-4137.
30. Oakley, G.G. and Patrick, S.M. (2010) Replication protein A: directing traffic at the intersection of replication and repair. *Front Biosci (Landmark Ed)*, **15**, 883-900.
31. Pike, A.M., Friend, C.M. and Bell, S.P. (2023) Distinct RPA functions promote eukaryotic DNA replication initiation and elongation. *Nucleic Acids Res*, **51**, 10506-10518.
32. Bochkareva, E., Korolev, S. and Bochkarev, A. (2000) The role for zinc in replication protein A. *J Biol Chem*, **275**, 27332-27338.
33. Lao, Y., Lee, C.G. and Wold, M.S. (1999) Replication protein A interactions with DNA. 2. Characterization of double-stranded DNA-binding/helix-destabilization activities and the role of the zinc-finger domain in DNA interactions. *Biochemistry*, **38**, 3974-3984.
34. Bochkareva, E., Korolev, S., Lees-Miller, S.P. and Bochkarev, A. (2002) Structure of the RPA trimerization core and its role in the multistep DNA-binding mechanism of RPA. *EMBO J*, **21**, 1855-1863.

35. Marechal, A. and Zou, L. (2015) RPA-coated single-stranded DNA as a platform for post-translational modifications in the DNA damage response. *Cell Res*, **25**, 9-23.
36. Mer, G., Bochkarev, A., Gupta, R., Bochkareva, E., Frappier, L., Ingles, C.J., Edwards, A.M. and Chazin, W.J. (2000) Structural basis for the recognition of DNA repair proteins UNG2, XPA, and RAD52 by replication factor RPA. *Cell*, **103**, 449-456.
37. Feldkamp, M.D., Mason, A.C., Eichman, B.F. and Chazin, W.J. (2014) Structural analysis of replication protein A recruitment of the DNA damage response protein SMARCAL1. *Biochemistry*, **53**, 3052-3061.
38. Wold, M.S. (1997) Replication protein A: a heterotrimeric, single-stranded DNA-binding protein required for eukaryotic DNA metabolism. *Annu Rev Biochem*, **66**, 61-92.
39. Fan, J. and Pavletich, N.P. (2012) Structure and conformational change of a replication protein A heterotrimer bound to ssDNA. *Genes Dev*, **26**, 2337-2347.
40. Bochkarev, A., Pfuetzner, R.A., Edwards, A.M. and Frappier, L. (1997) Structure of the single-stranded-DNA-binding domain of replication protein A bound to DNA. *Nature*, **385**, 176-181.
41. Iftode, C. and Borowiec, J.A. (2000) 5' --> 3' molecular polarity of human replication protein A (hRPA) binding to pseudo-origin DNA substrates. *Biochemistry*, **39**, 11970-11981.
42. Pestryakov, P.E., Khlimankov, D.Y., Bochkareva, E., Bochkarev, A. and Lavrik, O.I. (2004) Human replication protein A (RPA) binds a primer-template junction in the absence of its major ssDNA-binding domains. *Nucleic Acids Res*, **32**, 1894-1903.
43. Dornreiter, I., Erdile, L.F., Gilbert, I.U., von Winkler, D., Kelly, T.J. and Fanning, E. (1992) Interaction of DNA polymerase alpha-primase with cellular replication protein A and SV40 T antigen. *EMBO J*, **11**, 769-776.
44. Braun, K.A., Lao, Y., He, Z., Ingles, C.J. and Wold, M.S. (1997) Role of protein-protein interactions in the function of replication protein A (RPA): RPA modulates the activity of DNA polymerase alpha by multiple mechanisms. *Biochemistry*, **36**, 8443-8454.
45. Lisova, A.E., Baranovskiy, A.G., Morstadt, L.M., Babayeva, N.D. and Tahirov, T.H. (2022) Human DNA polymerase alpha has a strong mutagenic potential at the initial steps of DNA synthesis. *Nucleic Acids Res*, **50**, 12266-12273.
46. Wang, G. and Vasquez, K.M. (2014) Impact of alternative DNA structures on DNA damage, DNA repair, and genetic instability. *DNA Repair (Amst)*, **19**, 143-151.
47. Cea, V., Cipolla, L. and Sabbioneda, S. (2015) Replication of Structured DNA and its implication in epigenetic stability. *Front Genet*, **6**, 209.
48. Mirkin, E.V. and Mirkin, S.M. (2007) Replication fork stalling at natural impediments. *Microbiol Mol Biol Rev*, **71**, 13-35.
49. Qin, Y. and Hurley, L.H. (2008) Structures, folding patterns, and functions of intramolecular DNA G-quadruplexes found in eukaryotic promoter regions. *Biochimie*, **90**, 1149-1171.
50. Olson, C.L., Barbour, A.T., Wieser, T.A. and Wuttke, D.S. (2023) RPA engages telomeric G-quadruplexes more effectively than CST. *Nucleic Acids Res*, **51**, 5073-5086.
51. Salas, T.R., Petruseva, I., Lavrik, O., Bourdoncle, A., Mergny, J.L., Favre, A. and Saintome, C. (2006) Human replication protein A unfolds telomeric G-quadruplexes. *Nucleic Acids Res*, **34**, 4857-4865.
52. Nguyen, B., Sokoloski, J., Galletto, R., Elson, E.L., Wold, M.S. and Lohman, T.M. (2014) Diffusion of human replication protein A along single-stranded DNA. *J Mol Biol*, **426**, 3246-3261.
53. Chen, H., Lisby, M. and Symington, L.S. (2013) RPA coordinates DNA end resection and prevents formation of DNA hairpins. *Mol Cell*, **50**, 589-600.

54. Ambrus, A., Chen, D., Dai, J., Jones, R.A. and Yang, D. (2005) Solution structure of the biologically relevant G-quadruplex element in the human c-MYC promoter. Implications for G-quadruplex stabilization. *Biochemistry*, **44**, 2048-2058.
55. Hatzakis, E., Okamoto, K. and Yang, D. (2010) Thermodynamic stability and folding kinetics of the major G-quadruplex and its loop isomers formed in the nuclease hypersensitive element in the human c-Myc promoter: effect of loops and flanking segments on the stability of parallel-stranded intramolecular G-quadruplexes. *Biochemistry*, **49**, 9152-9160.
56. He, Q., Lin, X., Chavez, B.L., Agrawal, S., Lusk, B.L. and Lim, C.J. (2022) Structures of the human CST-Polalpha-primase complex bound to telomere templates. *Nature*, **608**, 826-832.
57. He, Y., Song, H., Chan, H., Liu, B., Wang, Y., Susac, L., Zhou, Z.H. and Feigon, J. (2022) Structure of Tetrahymena telomerase-bound CST with polymerase alpha-primase. *Nature*, **608**, 813-818.
58. Zhang, M., Wang, B., Li, T., Liu, R., Xiao, Y., Geng, X., Li, G., Liu, Q., Price, C.M., Liu, Y. *et al.* (2019) Mammalian CST averts replication failure by preventing G-quadruplex accumulation. *Nucleic Acids Res*, **47**, 5243-5259.
59. Zhang, Y., Baranovskiy, A.G., Tahirov, T.H. and Pavlov, Y.I. (2014) The C-terminal domain of the DNA polymerase catalytic subunit regulates the primase and polymerase activities of the human DNA polymerase alpha-primase complex. *J Biol Chem*, **289**, 22021-22034.
60. Ahmad, F., Patterson, A., Deveryshetty, J., Mattice, J.R., Pokhrel, N., Bothner, B. and Antony, E. (2021) Hydrogen-deuterium exchange reveals a dynamic DNA-binding map of replication protein A. *Nucleic Acids Res*, **49**, 1455-1469.
61. Baranovskiy, A.G., Babayeva, N.D., Lisova, A.E., Morstadt, L.M. and Tahirov, T.H. (2022) Structural and functional insight into mismatch extension by human DNA polymerase alpha. *Proc Natl Acad Sci U S A*, **119**, e2111744119.
62. Yuzhakov, A., Kelman, Z., Hurwitz, J. and O'Donnell, M. (1999) Multiple competition reactions for RPA order the assembly of the DNA polymerase delta holoenzyme. *EMBO J*, **18**, 6189-6199.
63. Cai, S.W., Zinder, J.C., Svetlov, V., Bush, M.W., Nudler, E., Walz, T. and de Lange, T. (2022) Cryo-EM structure of the human CST-Polalpha/primase complex in a recruitment state. *Nat Struct Mol Biol*, **29**, 813-819.
64. Jones, M.L., Baris, Y., Taylor, M.R.G. and Yeeles, J.T.P. (2021) Structure of a human replisome shows the organisation and interactions of a DNA replication machine. *EMBO J*, **40**, e108819.
65. Ganai, R.A., Bylund, G.O. and Johansson, E. (2015) Switching between polymerase and exonuclease sites in DNA polymerase epsilon. *Nucleic Acids Res*, **43**, 932-942.
66. Goswami, P., Abid Ali, F., Douglas, M.E., Locke, J., Purkiss, A., Janska, A., Eickhoff, P., Early, A., Nans, A., Cheung, A.M.C. *et al.* (2018) Structure of DNA-CMG-Pol epsilon elucidates the roles of the non-catalytic polymerase modules in the eukaryotic replisome. *Nat Commun*, **9**, 5061.
67. Xing, X., Kane, D.P., Bulock, C.R., Moore, E.A., Sharma, S., Chabes, A. and Shcherbakova, P.V. (2019) A recurrent cancer-associated substitution in DNA polymerase epsilon produces a hyperactive enzyme. *Nat Commun*, **10**, 374.
68. Eddy, S., Maddukuri, L., Ketkar, A., Zafar, M.K., Henninger, E.E., Pursell, Z.F. and Eoff, R.L. (2015) Evidence for the kinetic partitioning of polymerase activity on G-quadruplex DNA. *Biochemistry*, **54**, 3218-3230.
69. Barbour, A.T. and Wuttke, D.S. (2023) RPA-like single-stranded DNA-binding protein complexes including CST serve as specialized processivity factors for polymerases. *Curr Opin Struct Biol*, **81**, 102611.

70. Xie, S., Lu, Y., Jakoncic, J., Sun, H., Xia, J. and Qian, C. (2014) Structure of RPA32 bound to the N-terminus of SMARCAL1 redefines the binding interface between RPA32 and its interacting proteins. *FEBS J*, **281**, 3382-3396.
71. Arunkumar, A.I., Stauffer, M.E., Bochkareva, E., Bochkarev, A. and Chazin, W.J. (2003) Independent and coordinated functions of replication protein A tandem high affinity single-stranded DNA binding domains. *J Biol Chem*, **278**, 41077-41082.
72. Yates, L.A., Aramayo, R.J., Pokhrel, N., Caldwell, C.C., Kaplan, J.A., Perera, R.L., Spies, M., Antony, E. and Zhang, X. (2018) A structural and dynamic model for the assembly of Replication Protein A on single-stranded DNA. *Nat Commun*, **9**, 5447.
73. Loor, G., Zhang, S.J., Zhang, P., Toomey, N.L. and Lee, M.Y. (1997) Identification of DNA replication and cell cycle proteins that interact with PCNA. *Nucleic Acids Res*, **25**, 5041-5046.
74. Lisova, A.E., Baranovskiy, A.G., Morstadt, L.M., Babayeva, N.D., Stepchenkova, E.I. and Tahirov, T.H. (2022) The iron-sulfur cluster is essential for DNA binding by human DNA polymerase epsilon. *Sci Rep*, **12**, 17436.
75. Weeks, S.D., Drinker, M. and Loll, P.J. (2007) Ligation independent cloning vectors for expression of SUMO fusions. *Protein Expr Purif*, **53**, 40-50.
76. Liu, H. and Naismith, J.H. (2008) An efficient one-step site-directed deletion, insertion, single and multiple-site plasmid mutagenesis protocol. *BMC Biotechnol*, **8**, 91.
77. Gasteiger, E., Hoogland, C., Gattiker, A., Duvaud, S., Wilkins, M.R., Appel, R.D. and Bairoch, A. (2005) In Walker, J. M. (ed.), *The Proteomics Protocols Handbook*. . Humana Press, pp. 571-607.

TABLES

Table 1. Effect of the W-domain on RPAcore interaction with T:P and Polα/T:P.

RPA variant	Polα$_{CD}$	k_{off} x10^{-3} sec^{-1}	k_{on} mM^{-1} sec^{-1}	K_D [a] nM
RPAcore$^{\Delta P,W}$	-	24.6 ± 3.3	272 ± 22	90.2 ± 4.5
	+	266 ± 12.5	106 ± 9.5	2516 ± 108
RPAcore$^{\Delta P}$	-	28.7 ± 3.2	232 ± 9.1	124 ± 15
	+	5.7 ± 0.35	115 ± 19	50.3 ± 6.6

[a] K_D values are obtained by dividing k_{off} by k_{on}.
Data are presented as mean ±SD (n = 3).

FIGURE LEGENDS

Figure 1. A schematic representation of the domain organization of human RPA and its variants and the mode of RPA-DNA interaction. RPA contain six OB-folds (F, A, B, C, D, E) and four of them (A-D) participate in DNA binding. RPAcore is a complex of two small subunits with the C-domain of RPA70. The star symbol denotes a zinc-binding motif; P – phosphorylation motif; W – winged helix-turn-helix domain (wHTH). The deleted domains are depicted by a cross-hatching pattern.

Figure 2. RPA stimulates the primosome upon DNA synthesis across a hairpin. The 98-mer DNA templates of different structure were annealed to a 12-mer chimeric RNA-DNA primer containing the triphosphate at the 5'-end. The following template:primer combinations were used: T1:P1 (lanes 1-4), T2:P1 (lanes 5-8), and T3:P1 (lanes 9-12). The 5'-tails of T2 and T3 are prone to the formation of hairpin and G-quadruplex structures, respectively.

Figure 3. The role of RPA domains in DNA synthesis by primosome on normal and HP template. **(A)** The W-domain and the full DNA-binding capacity of RPA are important for HP bypass. DNA templates T1 (normal) and T2 (HP) were annealed to a 12-mer chimeric RNA-DNA primer (P1) containing the triphosphate at the 5'-end. (**B)** RPAcore$^{\Delta P,W}$ does not stimulate primosome on both templates. The 40-mer template (T4) was used to generate a 35-mer product (lane 1).

Figure 4. Polα requires intact RPA upon copying HP template. (**A**) RPA stimulates Polα_{CD} on HP but inhibits on G4 templates. DNA templates of different structure were annealed to a 16-mer DNA primer containing the Cy-5 fluorescent dye at the 5'-end. The following template:primer combinations were used: T5:P2 (lanes 1-5), T6:P2 (lanes 6-9), and T7:P2 (lanes 10-13). The 5'-tails of T6 and T7 are

prone to formation of hairpin and G-quadruplex, respectively. (**B**) The W-domain and DNA-binding domains of RPA are critical for HP bypass by Polα_{CD}.

Figure 5. DNA-binding studies of RPAcore$^{\Delta P,W}$ (A) and its variant with an intact W-domain (B) in the presence of Polα_{CD}. RPAcore$^{\Delta P}$ and its variant missing the W-domain dissociate from the DNA/Polα sensor in 15 min and 50 sec, respectively.

Figure 6. RPA does not help Polε upon copying HP and G4 templates. DNA templates of different structure were annealed to a 16-mer DNA primer containing the Cy-5 fluorescent dye at the 5'-end. The following template:primer combinations were used: T5:P2 (lanes 1-4 and 13), T6:P2 (lanes 5-8), and T7:P2 (lanes 9-12). The 5'-tails of T6 and T7 are prone to formation of hairpin and G-quadruplex, respectively.

Figure 7. RPAcore has potential for joint ssDNA binding with Polα. (A) Overall view of the aligned RPA/DNA and CST/Polα/DNA complexes. DNA is shown as sticks. (**B)** Close-up view of DNA-binding clefts of CST and RPA. DNA is shown as a cartoon. CST and Polα are colored gray and slate, respectively. The RPA domains C, D, and E are colored green, cyan, and pink, respectively. The carbons of DNA from the complexes with CST and RPA are colored yellow and orange, respectively. For clarity, the N-terminal parts of CTC1 (aa 1-544) and of the large subunit of RPA (aa 1-447; this part is distant from Polα) are not shown, and the α-helix of STN1 (aa 104-123) is shown with 50% transparency. Of the four primosome subunits, only Polα_{CD} is shown. RPA from the fungus *Ustilago maydis* bound to ssDNA (pdb code 4gnx) was superimposed onto the CST/Polα/ssDNA complex (pdb

code 8d0b), using domains C and D for alignment. PyMol Molecular Graphics System (version 1.8, Schrödinger, LLC) was used for figure preparation.

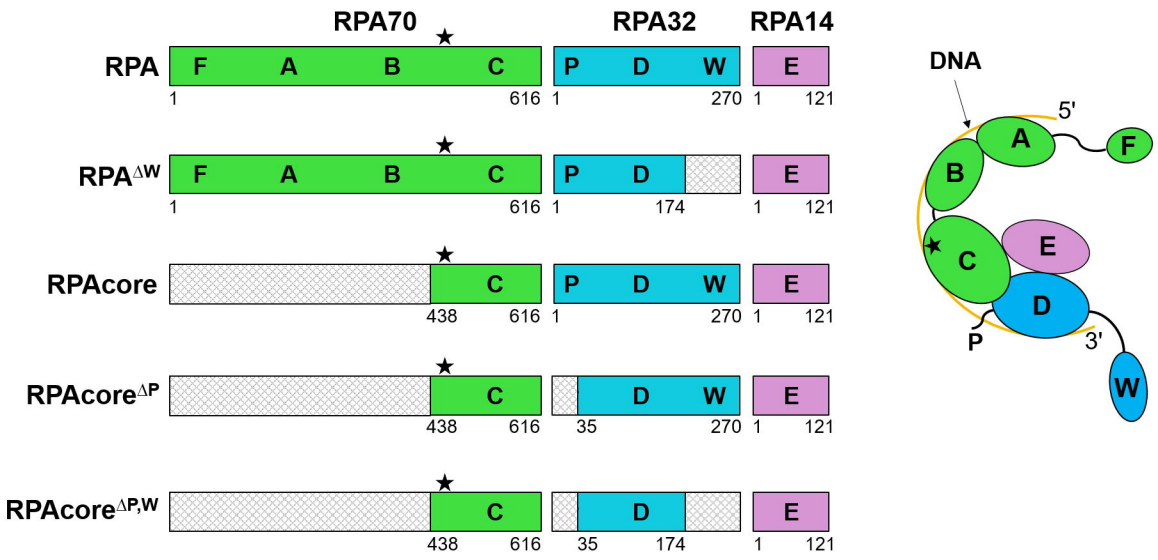
RPA70
RPA32
RPA14
RPA
F
A
B
C
P
D
W
E
1
616
1
270
1
121
RPA^ΔW
1
616
1
174
1
121
RPAcore
438
616
1
270
1
121
RPAcore^ΔP
438
616
35
270
1
121
RPAcore^ΔP,W
438
616
35
174
1
121
DNA
5'
3'
A
F
B
C
E
D
P
W

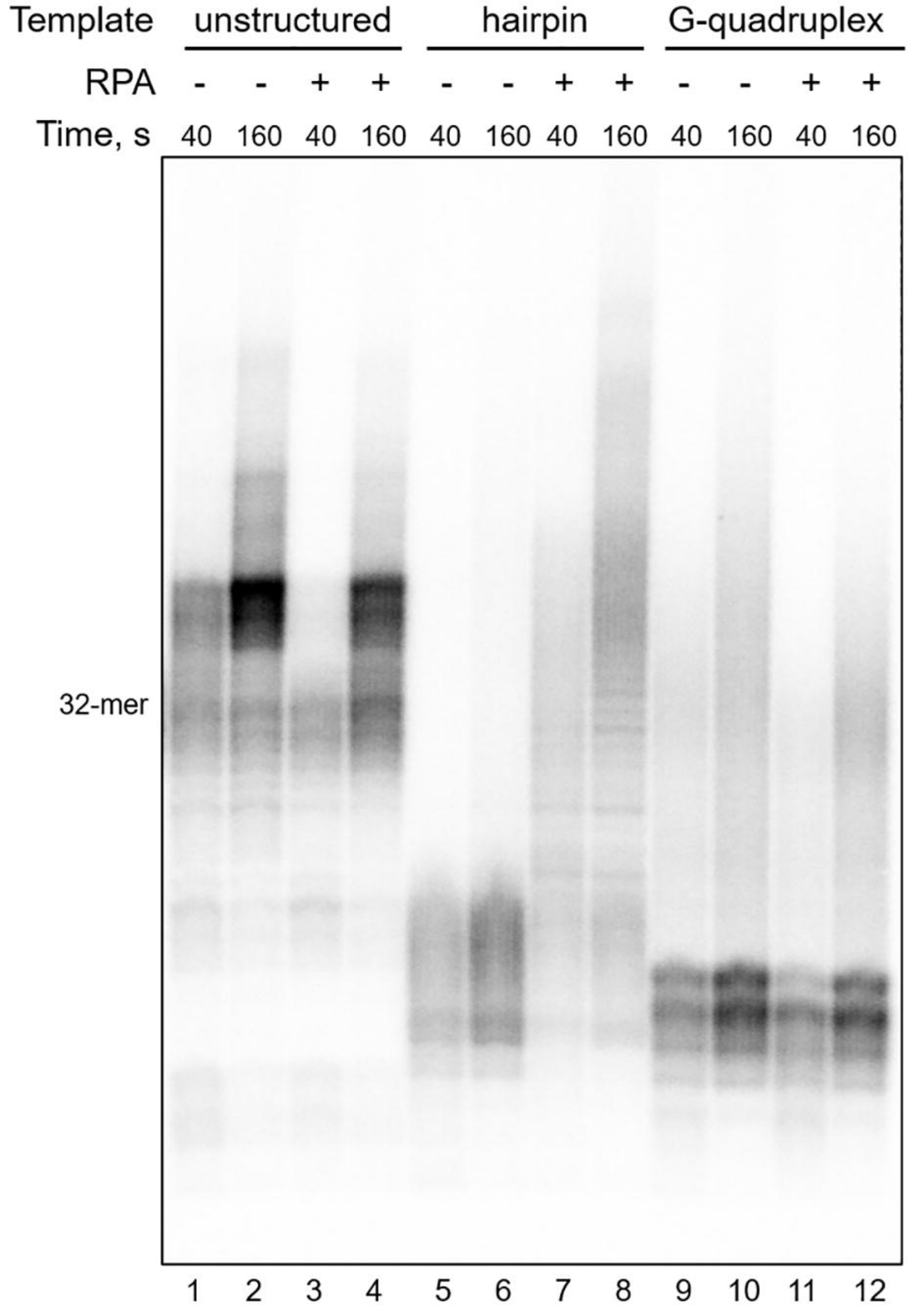
Template
unstructured
hairpin
G-quadruplex
RPA
- - + + - - + + - - + +
Time, s
40 160 40 160 40 160 40 160 40 160 40 160
32-mer
1 2 3 4 5 6 7 8 9 10 11 12

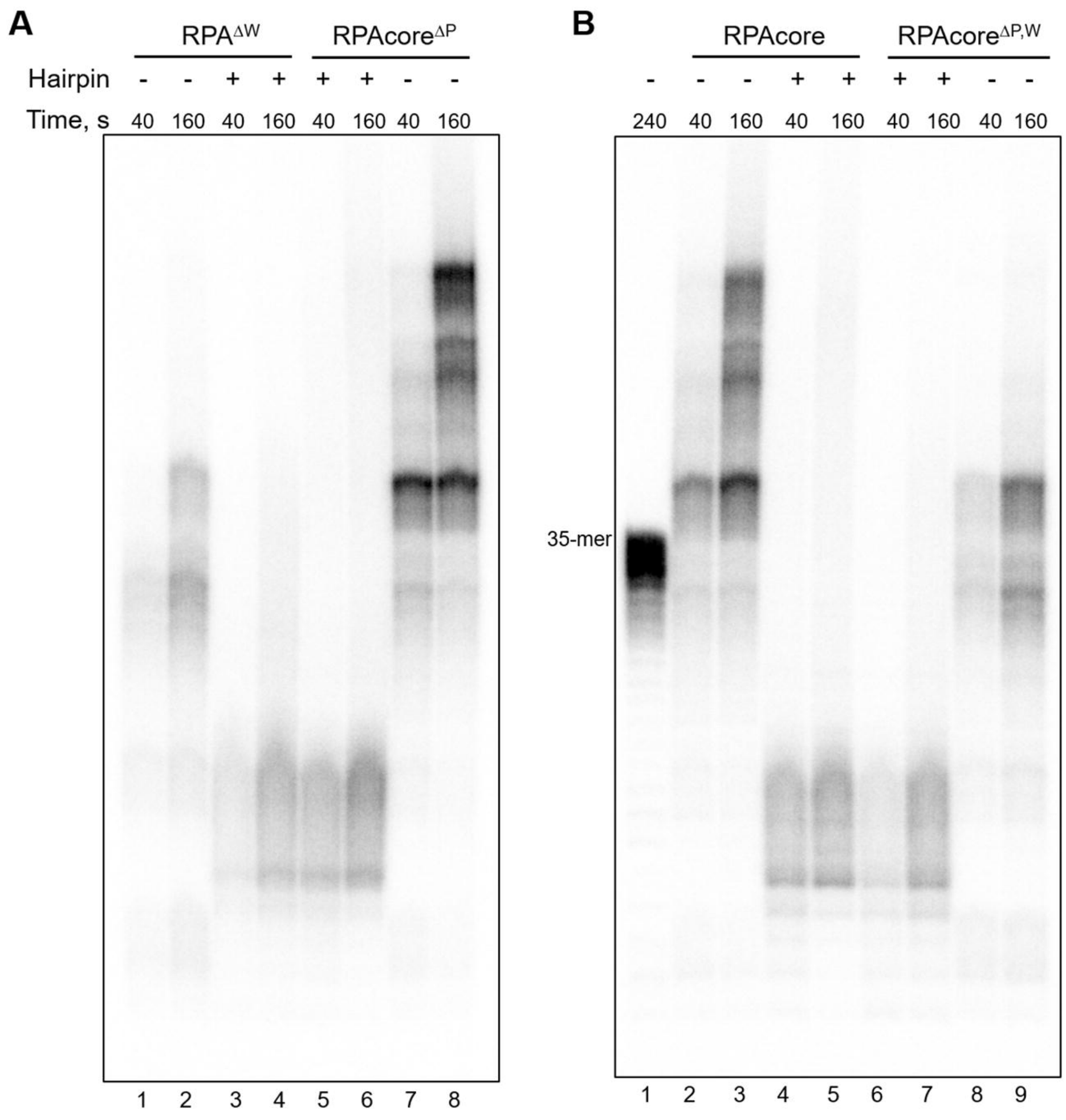
A
RPA$^{\Delta W}$
RPAcore$^{\Delta P}$
Hairpin - - + + + + - -
Time, s 40 160 40 160 40 160 40 160
1 2 3 4 5 6 7 8
B
RPAcore
RPAcore$^{\Delta P,W}$
- - - + + + + - -
240 40 160 40 160 40 160 40 160
35-mer
1 2 3 4 5 6 7 8 9

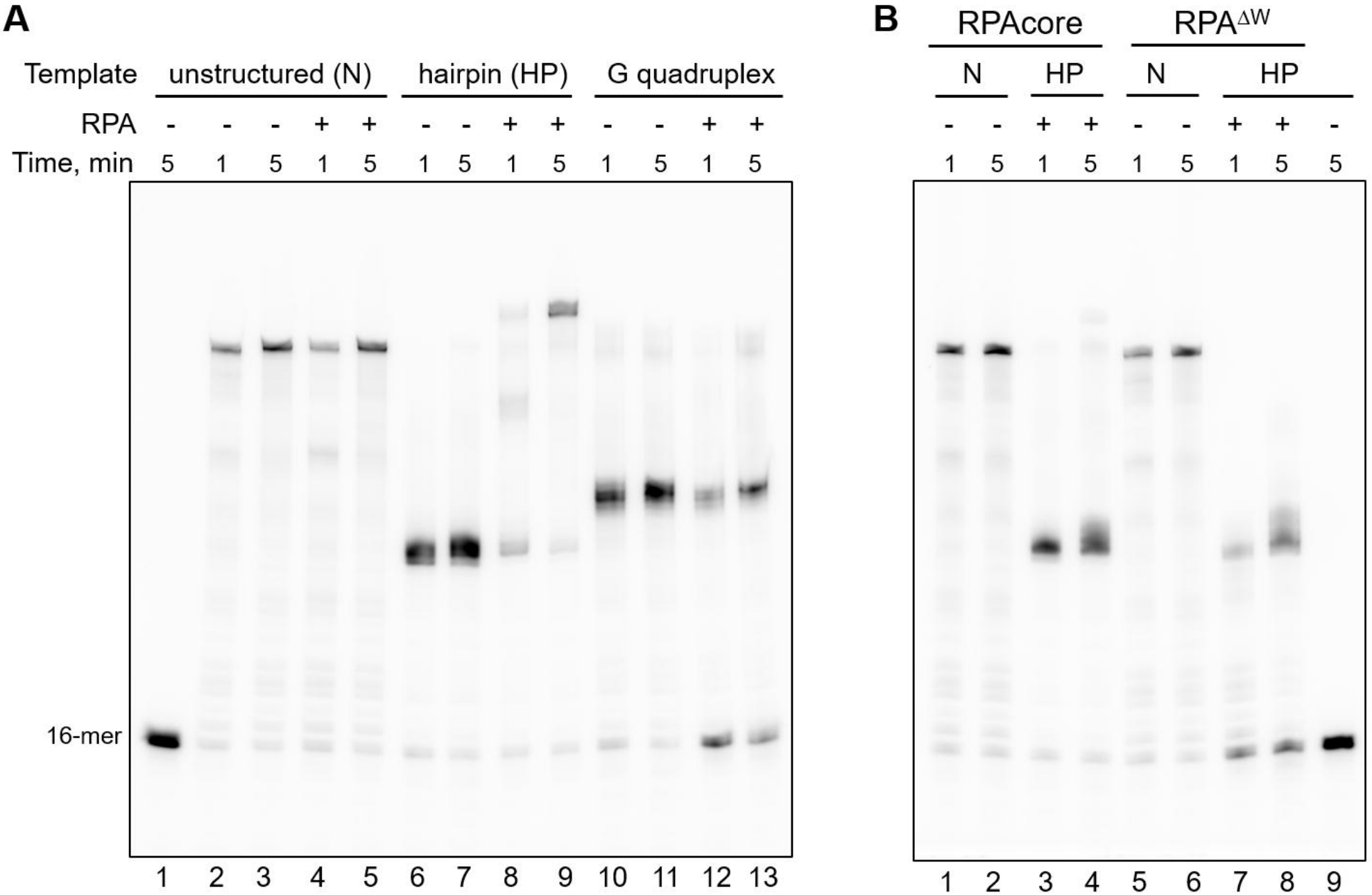
A
Template
unstructured (N)
hairpin (HP)
G quadruplex
RPA
- - - + + - - + + - - + +
Time, min
5 1 5 1 5 1 5 1 5 1 5 1 5
16-mer
1 2 3 4 5 6 7 8 9 10 11 12 13
B
RPAcore
RPA$^{\Delta W}$
N
HP
N
HP
- - + + - - + + -
1 5 1 5 1 5 1 5 5
1 2 3 4 5 6 7 8 9

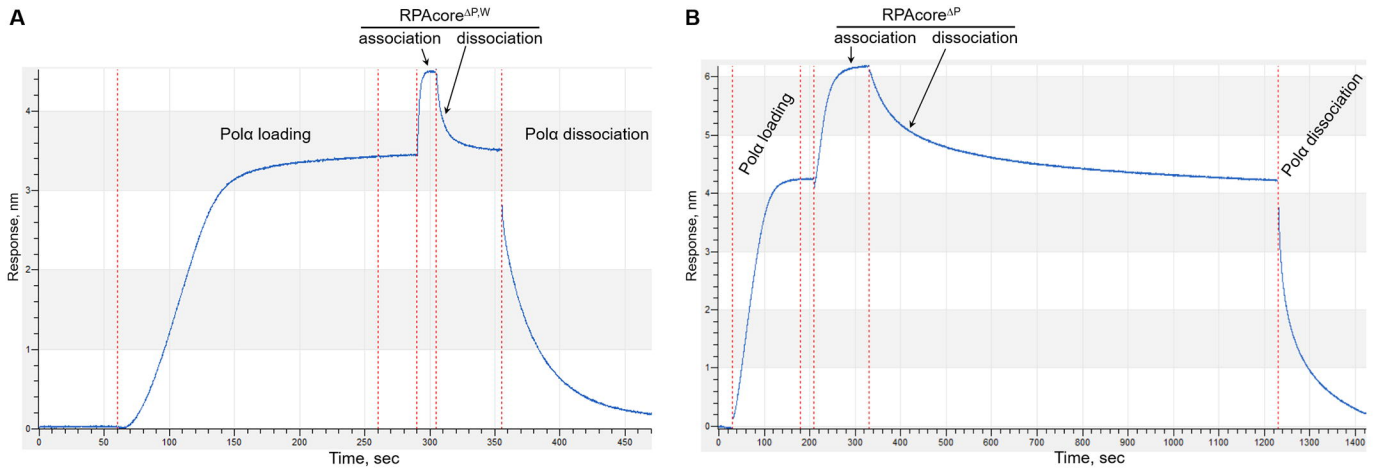
A
RPAcore$^{\Delta P,W}$
association
dissociation
Polα loading
Polα dissociation
Response, nm
Time, sec
B
RPAcore$^{\Delta P}$
association
dissociation
Polα loading
Polα dissociation
Response, nm
Time, sec

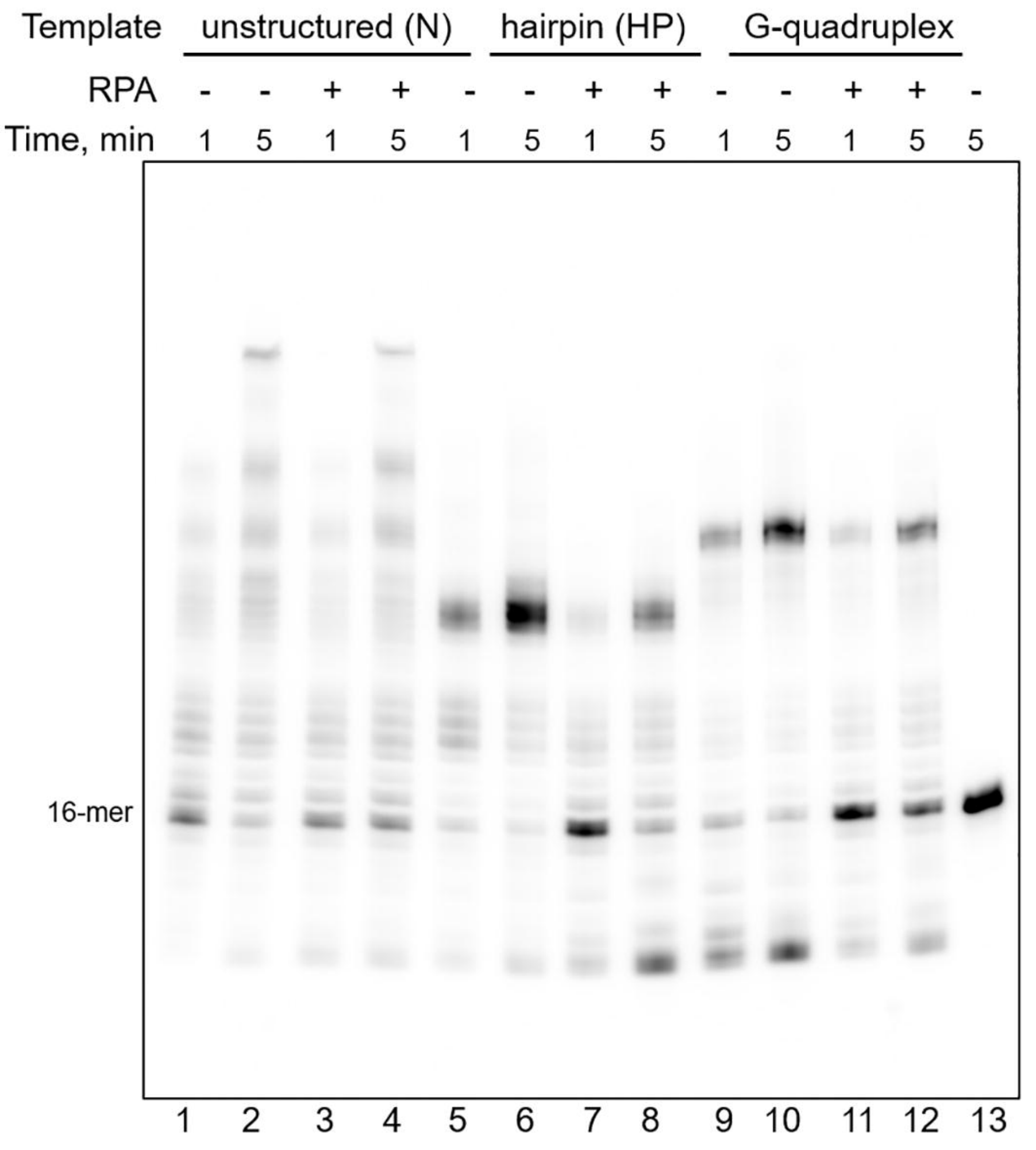
Template
unstructured (N)
hairpin (HP)
G-quadruplex
RPA
- - + + - - + + - - + + -
Time, min
1 5 1 5 1 5 1 5 1 5 1 5 5
16-mer
1 2 3 4 5 6 7 8 9 10 11 12 13

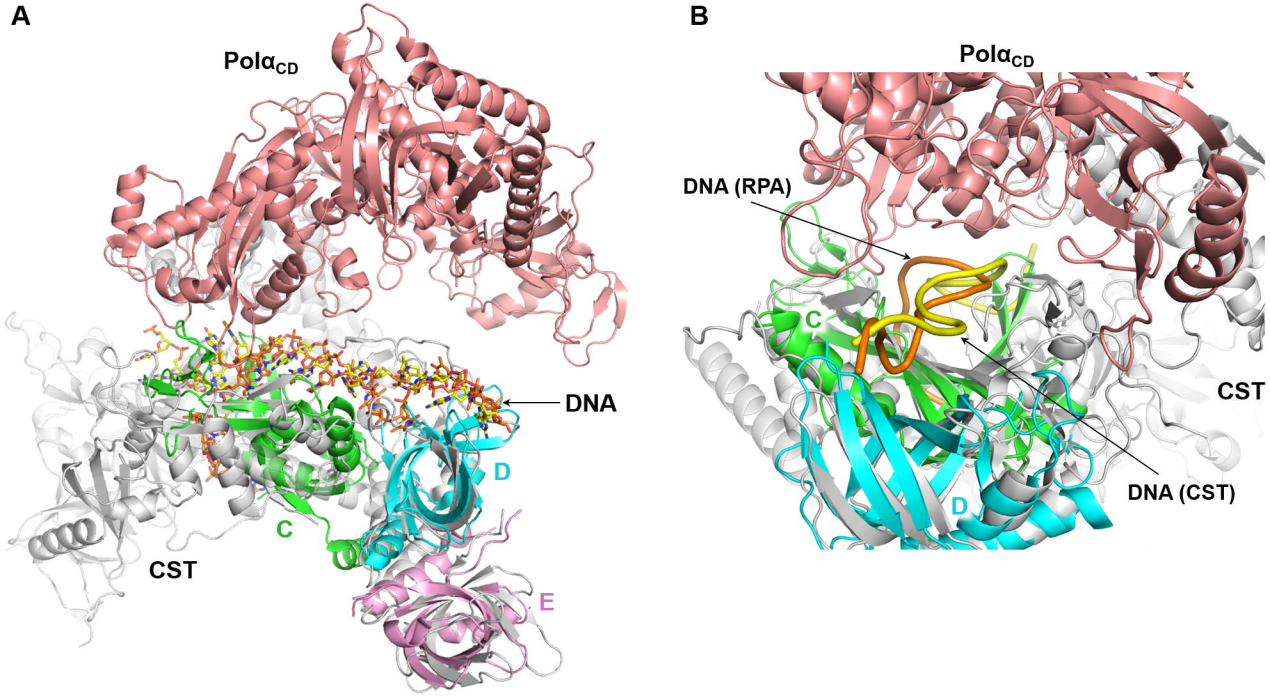
A
Polα$_{CD}$
DNA
D
C
CST
E
B
Polα$_{CD}$
DNA (RPA)
C
CST
DNA (CST)
D